BACKGROUND

Microarray analysis enables disease diagnosis and detection of a large number of mutations in selected genes from individuals, faster, more economically, and more comprehensively than has been previously possible. More diseases have been found to have a genetic link than were previously thought and the significance of monitoring mutations and other variants in important genes has become increasingly vital. Rapid and automated screening of a large number of genetic abnormalities in individuals has led to a deeper understanding of genetics and disease processes. For example, 57 genetic mutations of the BRCA1 gene have been found, which are known to increase susceptibility to breast and ovarian cancer [1].

Description of Sequence Analysis with Microarrays

Sequence analysis with microarrays begins with immobilization of a set of oligodeoxy-nucleotides (ODNs) of known sequences to a solid surface or, alternatively, synthesis of an array of ODNs *in situ* on the surface. Labeled target DNA or RNA fragments, whose sequences are unknown, are applied to the chip in a buffer solution and the those fragments containing sequences complementary to that of ODNs on the chip are allowed to hybridize. Hybridization between two complementary DNA strands produces a double-stranded helix in which the strands are antiparallel and joined through hydrogen bonds. Hybridization occurs over a matter of minutes to a few hours as the two strands are annealed at a temperature below the melting temperature for the duplex (T_m), which is influenced primarily by the types of base pairs and the stacking interaction between bases. Any base pair combination between the DNA strands other than AT and GC (Watson-Crick rules) is termed mispairing and causes destabilization between the DNA strands [2]. Following hybridization, the presence of the label (typically a dye) at a site on the surface indicates that the DNA contains the complementary sequence to the ODN at that site.

Some of the variables in this type of sequencing are the length and composition of the ODN, the length of the DNA/RNA fragment, the method of labeling and detection of the hybridization, and the conditions for hybridization. Using this method of sequence analysis, DNA can be assessed for the presence of a large number of short defined sequences.

Sequencing using an ODN array was originally conceived as a method of determining DNA sequence by hybridizing the DNA to a complete set of ODNs that represent all possible

combinations of the four nucleotides that constitute DNA, e.g., there would be 4^8 combinations in a set of octamers. With such an ODN matrix, which may be on the order of 1-cm x 1-cm in size, a single DNA fragment may be evaluated over the entire set of ODN sequences simultaneously by noting the positions in the matrix where target DNA is detected after hybridization. For medical diagnostics, abbreviated versions of the matrix are sufficient to detect a given mutation or alteration in DNA. Hundreds of short ODNs containing known mutations for a specific disease, can be located in different positions on a sequence analysis chip. Following hybridization, the bound labels are detected, thus diagnosing disease predisposition or genetic abnormality.

Glass, quartz, silicon, platinum and gold are all good surfaces for sequence analysis using ODN arrays and binding of ODN molecules to the surfaces is easily accomplished [3,4,5,6]. Fodor *et al.* developed a more efficient method of producing ODN array sequencing chips using light-directed, spatially addressable parallel ODN synthesis [7]. Using spatially localized deprotection, ODNs can be synthesized *in situ* in a checkerboard array. A density of 409,600 synthesis sites in a 1.28 cm x 1.28 cm array can be produced in which each 20μm x 20μm site contains ~4 x 10^6 copies of a specific ODN probe. The same technique has been used to prepare a high-density array consisting of over 96,600 ODNs to screen for a wide range of mutations on exon 11 of the hereditary breast and ovarian cancer gene, BRCA1 [8]. Arrays are now even being produced on a commercial basis.

Advantages of Using Microarrays for Sequence Analysis

Because of the parallel nature of information obtained from them, ODN arrays can be used to screen for multiple genetic mutations simultaneously. A few genetic disorders, such as sickle cell disease and achondoplasia have only one mutation associated with them for different affected individuals. More commonly, however, extensive heterogeneity of mutations is observed. For example, more than 225 possible disease-causing mutations have been identified for cystic fibrosis [9]. Although cystic fibrosis is the most frequently inherited disease in the West, with an incidence of 1 in 2500, genetic diagnosis has been difficult due to the large number of possible mutations [10]. There is no known way other than DNA analysis to detect cystic fibrosis carriers, which have a frequency of 1 in 25 among Caucasians. Detection of the mutations with ODN arrays has the potential to significantly improve diagnosis and genetic

counseling. Five hereditary forms of Alzheimer's disease have been identified, with mutant genes located on chromosomes 19, 21, 14, and 1 [11,12]. Determining the heterozygous chromosomes can help to determine the age of onset and the rate of the development of the disease. In other diseases, knowledge about the combination of risk-associated and protective genes can establish a risk factor for that disease in a particular person, as in Type-1 Diabetes [13]. From these examples, it is evident that a very significant characteristic of genetic testing based on ODN arrays is the capability to screen for multiple mutations simultaneously.

The Problems Associated with Present Methods of Probe Density Analysis

Currently, the most common method of detecting a DNA fragment that has been hybridized to a bound ODN is by labeling the DNA fragment with a fluorescent reporter group prior to hybridization, and then using a confocal microscope to detect fluorescence of the label at the location of hybridization. Although fluorescence detection has been adequate for analysis of the hybridized chips, it is unsuitable for some aspects of chip development and production. For example, it would be useful to have a high-resolution image of DNA hybridized to a small area of bound ODNs (spot sizes as small as 10-μm can be made on an array). This would allow tests of the homogeneity of the bound ODN and determine if there are any edge effects that influence hybridization efficiency. Fluorescence detection does not have the spatial resolution to perform these studies nor the dynamic range to perform hybridization kinetics studies.

Various methods of attaching the probes produce differing quantities of attached molecules. ODNs can be prepared by automated synthesis and then immobilized on surfaces in an array using many different methods with varying degrees of efficiency [14,15,16,17]. Arrays can also be created by *in situ* photolithographic techniques [18]. *In situ* synthesis methods face a unique issue, that of step yield (the amount of product correctly synthesized). The step yield is lower for *in situ* methods, perhaps even reducing the length of ODNs that can be produced using these methods to 30 bases [19]. A high dynamic range, quantitative measurement method is needed to study parameters that increase efficiency and new methods of array production. With such a tool, a systematic study of hybridization strategies could be undertaken which would almost certainly lead to improved efficiencies and lower array manufacturing costs.

Resonance Ionization Detection of Sn-Labeled ODNs

The use of resonance ionization (RI) as a detection methodology offering superior spatial resolution and dynamic range has been investigated at Atom Sciences, Inc. In RI, tunable lasers are used to sequentially excite and then ionize atoms for the analysis of elements. The ions generated are detected with mass spectrometry. The energy spectrum of discrete excited states is unique to each element, so that selection of particular excited states for RI analysis provides great elemental selectivity. Previous research by Atom Sciences has demonstrated the basic operation of a Sputter-Initiated Resonance Ionization MicroProbe (SIRIMP) instrument that can detect DNA fragments labeled with stable isotopes [20, 21]. This technique combines RI with ion sputtering and mass spectrometry to provide a unique analytical capability. In previous DNA measurements, SIRIMP has been used in a qualitative manner to determine the existence or absence of a labeled DNA. However, SIRIMP should provide an effective tool to quantitatively determine probe densities because it avoids many of the disadvantages of other surface measurement techniques [22,23,24]. For example, nonresonant and electron-impact secondary neutral mass spectrometry (SNMS) lack the sensitivity and selectivity inherent to SIRIMP. Secondary ion mass spectrometry (SIMS) has poorer efficiency and sensitivity than SIRIMP and SIMS also suffers from matrix effects and isobaric interferences. Because SIRIMP uses a selective technique to ionize neutral atoms away from the surface, it is not subject to the types of interferences or the matrix effects of SIMS. The lack of interferences and extremely low noise levels inherent to SIRIMP also allows much greater dynamic range than is possible in SNMS or SIMS. Atom Sciences, Inc. has demonstrated measurements of concentrations varying by more than 6 orders of magnitude.

RI requires free atoms in the gas phase and in the SIRIMP technique, a pulsed ion beam is used to sputter constituents from the surface of a solid sample. The expanding cloud of sputtered material, mostly neutral particles, is probed by the RI laser beams that ionize all the atoms of the selected element within the volume intersected by the laser beams. Suppression of secondary ions produced by the sputtering process is achieved by a combination of the relative timing between the ion sputtering pulse and the firing of the RI lasers, timed extraction voltage switching, and electrostatic energy analysis. The ions are then detected in a TOF mass spectrometer. The mass spectrometer is added to the detection system to confirm the elemental identity of the ionized atom and/or to add isotopic identification.

For high spatial resolution, a liquid metal ion gun can be used which has a spot size of less than 0.1 μm. Vibrations reduce the resolution to a few tenths of a micrometer.

The selection of particular excited states for RI analysis provides great elemental selectivity. We previously demonstrated that the ionization efficiency for the selected element can be as much as 10^9 times higher than for the other elements in the sample **[**25**].** Since the isotope shifts of most elements are small in comparison to the bandwidth of the RI lasers used in our experiments (7-12 GHz), all isotopes of a chosen element will be ionized with essentially equal sensitivity. If a time-of-flight mass spectrometer (TOFMS) is used, all isotopes of an element can be detected simultaneously. One of the advantages of the TOFMS instrument is that multiple ODNs labeled with different isotopes can be measured simultaneously. Each of eight target DNA sequences can be labeled with a separate tin isotope, hybridized to DNA on a chip and detected using the SIRIMP detection method.

The unique selectivity of RI reduces the mass resolution requirements of the TOFMS to the resolution of neighboring isotopes; the high ionization selectivity of RI and the suppression of the secondary ions virtually eliminate interferences from molecular ions, isobars, or scattered ions from the major constituents of the sample. This property can be exploited for sequence analysis with ODN arrays. Only the specified element is detected, so background is limited to contamination by that element. Background can be minimized by proper attention to the purity of reagents and matrix surfaces. The effect of the background can be decreased even further by using one less enriched label than the number of isotopes for each element. The presence of the missing isotope then provides a direct measure of contamination, which can be subtracted from the measured value. The reduced background, combined with the surface sensitivity of RI analysis, allows precise measurements of the degree of hybridization that occurs for complementary and non-complementary DNA/ODN groups.

RIS Instrumentation

Atom Sciences' SIRIS instrument is composed of an Atomica Microfocus ion gun for atomization, two Nd:YAG laser pumped dye lasers, and a time-of-flight (TOF) mass spectrometer. To resonantly ionize tin, a ultraviolet (UV, 286.332 nm) + visible (VIS, 614.965 nm) +infrared (IR, 1.064 μm) laser scheme was used. The two bound-bound transitions (UV and VIS) and the ionization step (IR) can be saturated, as evidenced by the insensitivity of the signal

amplitude to small changes in the individual laser beam intensities. This assures near unit probability of ionizing all ground-state Sn atoms in the laser beam and simplifies calibration. The combination of relatively low laser intensities required to saturate bound-bound transitions and the use of an infrared wavelength for the ionization step, reduce nonresonant interferences from molecules, molecular fragments, or other elements. The bandwidth of the laser beam has been measured previously to be ~8-12 GHz. This ensures that all Sn isotopes (isotope shift << 7 GHz) and almost all velocity components are ionized with essentially equal sensitivity. The TOF mass spectrometer allows simultaneous detection of all isotopes.

For all measurements, the wavelength stability of the two tunable lasers was monitored using solid Fabry-Perot interferometers. Sn signals were integrated over the five major isotopes (amu 116-120) and an additional area of equal width was integrated to serve as baseline subtraction.

Analysis of Microarrays Produced by Photolithography

Samples were constructed by Affymetrix, Inc. on a 3"x 3" glass slide using their patented photolithographic *in situ* technique. One side was coated with a silane film and a hexaethylene oxide linker was attached in a circular region, approximately 2.4-cm in diameter, near the center. The 12.8-mm x 12.8-mm pattern shown in Figure 1 was constructed in the middle of this circle using light activated chemistry. This involved removing exposed photolabile protecting groups by directing light through a photolithographic mask to specific areas of the glass. The surface was then incubated with adenosine nucleosides, also bearing a photolabile protecting group. The nucleoside couples to the sites that have been exposed to light and, after several steps, an array of ODNs is formed. 3-Tributylstannyl cyanoethylphosphoramidite (Sn-CEP; [26-28]), synthesized by ChemGenes Corporation (Waltham, MA; structure shown in Figure 2), was attached at the last step so the amount of Sn should be an accurate measure of the full n-mer at the site (the phosphoramidite will not bind to sites that have been capped off).

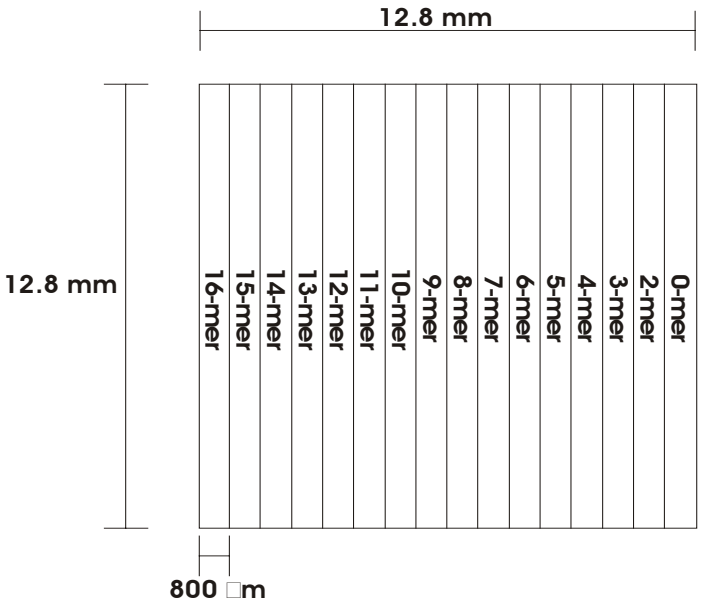

Figure 1. Pattern of in situ ODNs used for tests.

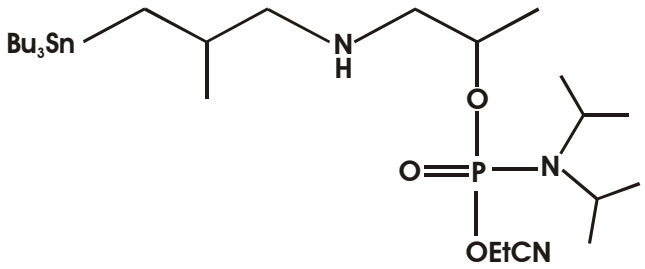

Figure 2. Structure of Sn-labeled phosphoramidite (3-Tributylstannyl cyanoethylphosphoramidite; Sn-CEP), which was used to label patterned ODN arrays described above.

The signal just off the ends of the area where the ODNs were constructed had a large background of Sn. Off the 16-mer end, the baseline signal was about 4.05 and sloped downward slightly as the surface probe moved farther from the ODN stripes. This baseline slope may be an instrument artifact but it was much smaller than the slope in **Figure 3** and therefore the change in signal in **Figure 3** is related to the change in ODN length.

An interesting effect was observed as we continued to analyze this same sample. After several hours in vacuum, the Sn signal diminished significantly (see Figure 4). If fact, as we analyzed off the 16-mer end of the ODN area, the background levels, which were similar in magnitude to that described above in the previous analysis, were actually larger than the Sn signal from the ODNs.

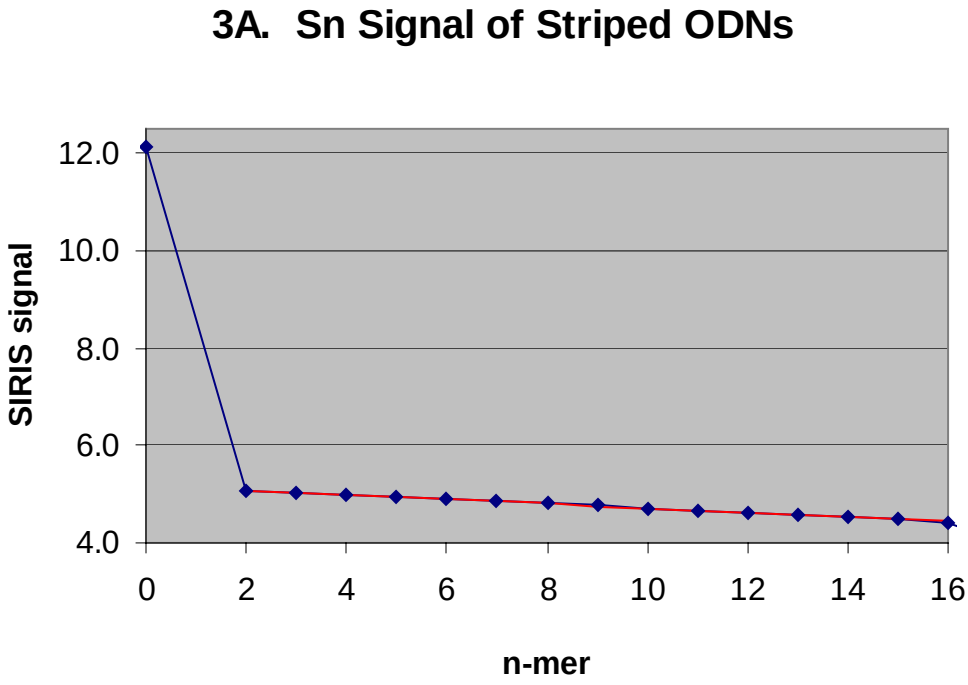

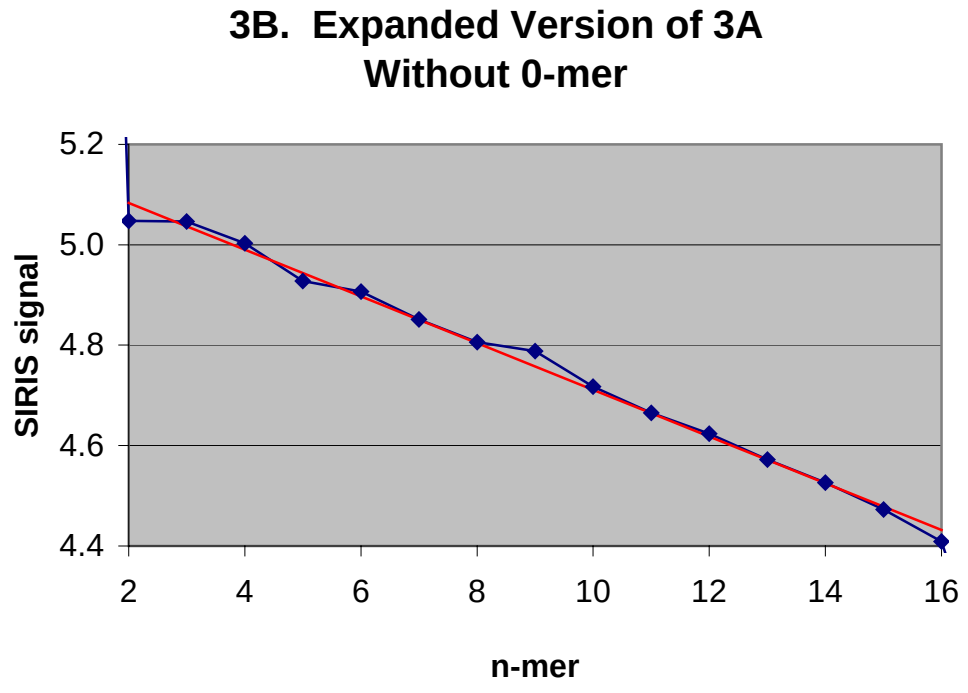

Figure 3. Data from SIRIS analysis of Sn on striped ODNs formed by photolithography. 3B is the same data as 3A but without the 0-mer. Linear fit shown in red (ignoring the 0-mer).

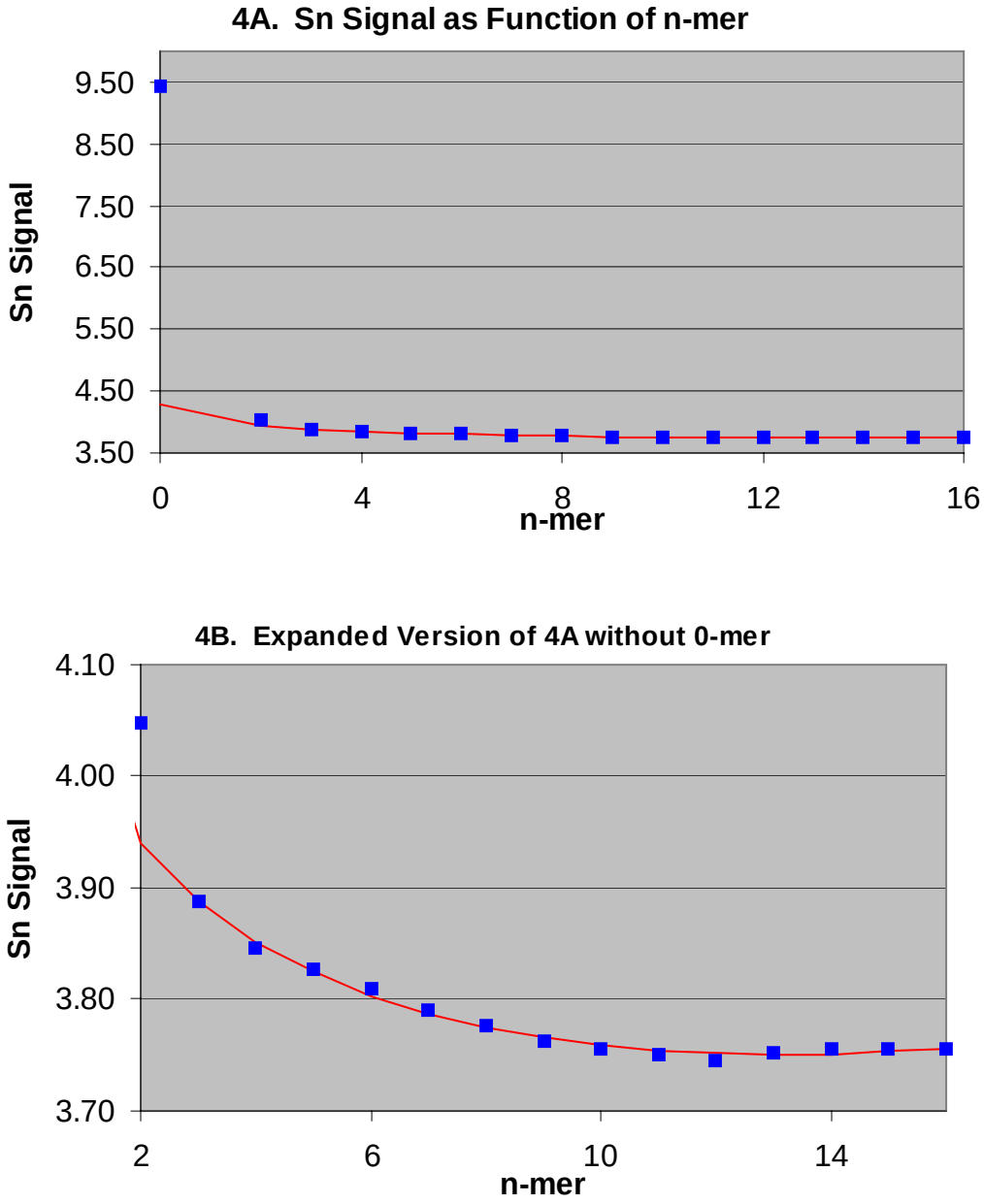

Figure 4. SIRIS analysis of Sn-labeled ODNs. This is a repeat of the analysis shown in Figure 3 except after several hours in the vacuum system. An exponential fit (red line) to the n-mer>2 data is shown.

This loss of signal was surprising because the Sn-labeled phosphoramidite should be covalently bound to the ODNs, which are covalently bound to the surface. Perhaps some fraction of the Sn-labeled phosphoramidite was not covalently bound but was physically held with

adequate attraction to withstand washings. If these non-covalently bound molecules were volatile, it might explain the loss of signal. We later performed tests on a similar compound, tin, 3-(triethylstannyl) propanoic acid (TESPA), and discovered it was quite volatile when deposited on a surface (not chemically bound) and inserted into a vacuum system. These results eventually led us to employ a different label other that Sn compounds.

After several months into Phase II, Affymetrix informed us that they had further developed fluorescent methods and that they no longer had an active interest in our resonance ionization technique. This was communicated to the program manager and it was decided that the project would continue and be focused on printed ODNs.

Analysis of Printed Oligodeoxynucleotides

We contracted Chemsyn Science Laboratories (Lenexa, Kansas) to synthesize 500 mg NHS-TESPA (1.6 g delivered) and a portion of the product was sent to Commonwealth Biotechnologies in Richmond, VA to label ODNs so that Sn-TESPA was attached at one end and a hexylamine linker was at the other. The procedure involved a 0.2 μmol oligonucleotide synthesis on a Model 8909 Expedite DNA synthesizer using a 3' amino modifier as the CPG support column. The synthesis was completed with the DMT group left on the 5' end. The 5' amino modifier was not added during the initial synthesis on the CPG, only the DNA bases. The synthesized oligo was not cleaved from the CPG at this step. TESPA addition was carried out on the oligo while it was still attached to the CPG as follows: 650 μl of dimethyl formamide, 50 μl of triethylamine, and 300 μl of NHS-TESPA were mixed in a reaction vial. This was then taken up by a 1-ml syringe which was then placed into the end of the synthesis column and another 1-ml syringe was placed on the other end. The TESPA conjugation mix was then pushed through the column several times between the two syringes. The conjugation was allowed to take place overnight with occasional agitation between the syringes. After conjugation, the NHS-TESPA was quenched by flushing the column with 2 mls of N-propylamine. After quenching, the column was flushed thoroughly with acetonitrile. The column was then placed back onto the synthesizer and the 5' hexylamine group was added. The complete oligo was then cleaved from the CPG support in ammonium hydroxide and deprotected at 55 degree C overnight. After completed synthesis, the oligo was purified by HPLC and run on a polyacrylamide gel to verify

which fraction contained the TESPA-labeled oligo. Three labeled oligos were synthesized in this fashion. They were:

A = 5'Hexylamine-TAATACGACTCACTATAGGG-3" NHS-TESPA

B = 5'Hexylamine-TACCAGAAGGCCAACGGGGG-3" NHS-TESPA

C = 5'Hexylamine-TTGCCTGAGTGCAGTATGGT-3" NHS-TESPA

Attachment of the labeled ODNs was performed by linking a uniform epoxide layer to a clean Si surface using an epoxysilane reagent and standard SiO_2 modification chemistry. Secondary amine formation with the epoxide ring provides the means to link the hexylamine-modified probes to the surface. A series of chips were prepared using 0.5x0.5 inch SiO_2 squares cut from a standard 4" diameter wafers. These were cleaned with 1M HNO_3 for 30 minutes and then rinsed with deionized water. The chips were then sonicated in baths of hexane, acetone, and methanol for 10 each, with deionized water rinses between each. After a final sonication in deionized water, the chips were allowed to dry. An epoxysilane solution was prepared in an argon-filled glovebox from 14 ml anhydrous xylene, 4 ml 3-glycidoxypropyltrimethoxysilane, and 0.5 ml N,N-diisopropylethylamine. The chips were allowed to soak overnight at room temperature in this solution. They were then rinsed several times with tetrahydrofuran and allowed to dry.

Stock solutions were made of the three oligos synthesized by Commonwealth Biosystems. These solutions were [A]=302 μM, [B]=88 μM, and [C]=80 μM. Absorption measurements were made at 260 nm with a UV spectrophotometer to confirm the concentrations. These measurements indicated the absorption was higher than would be predicted for the calculated concentrations, probably because of strong absorption by the Sn label. Dilutions by factors of 5, 10, and 20 were also made. For initial work, these concentrations were spotted by handheld pippette onto the epoxide surface of the prepared SiO_2 chips and the chips were then kept in a humid atmosphere at 60 degree C overnight. This produced spots varying in size and volume (typically about 1-mm in diameter), which were initially visible (before washing). Their location was marked with a diamond scribe well away from the actual spot position so that the intersection of the marks gave the location of the immobilized ODN. After washing in triethylamine and deionized water, the chips were dried and analyzed.

The measured background Sn was quite high in all the immobilized samples. The background was distinctly larger near the scribe marks, indicating that the one of the lower surfaces exposed by the scribe was the source of background. However, significant signal was observed throughout the samples. Figure 5 shows two scans over the 88-μM Oligo B spot in one sample. The background here is about 10% of the peak height and is relatively small and constant compared to many locations on the chips. The second scan in Figure 5 is about 10% greater in amplitude that the first scan. This was observed on most of the peaks when a second scan was performed over the same location as the first and is due to removal of "debris" during the first scan. SIRIMP is a surface analysis and any material covering the analyte will reduce or even eliminate the signal. For the data in this figure, the signal from 600 laser pulses was averaged at each point. Our ion beam produces about 650 nA and is pulsed on for 600 ns before the laser is fired in these experiments. This corresponds to about 2.4×10^6 ions per pulse. In a 60-μm x 120-μm elliptical spot, this corresponds to almost 9×10^{10} ions per cm^2. At this dose, it would take about 20,000 pulses to erode a single monolayer (assuming a sputter yield of 0.5 to 1). We performed a depth profile to determine how quickly the signal from the Sn labeled ODNs would disappear. This is shown in Figure 6. There is a fairly steep increase at the surface, indicating that 15 to 20% signal increase could be obtained by prerastering the sample. Although this increase is fully realized by the second datum in this plot, the

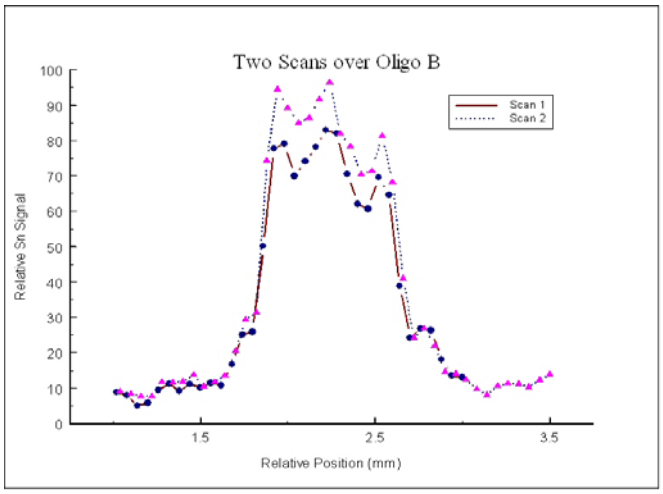

Figure 5. Two sequential SIRIS line scans over ODN-B.

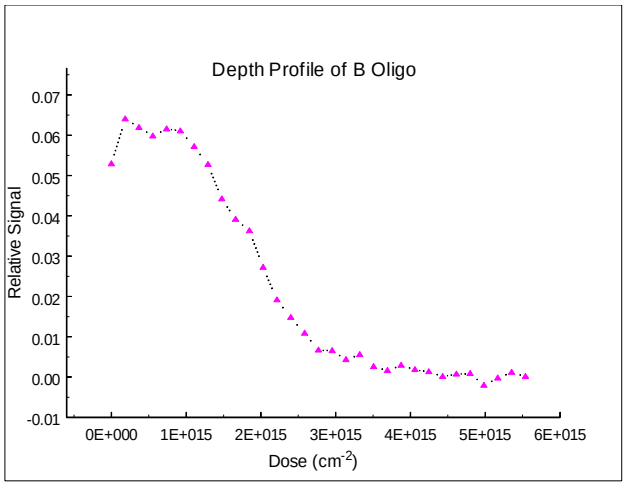

Figure 6. SIRIS profile as a function of primary ion beam dose.

data from the previous figure suggests that a dose of about $1x10^{14}$ ions per cm^2 would reach the maximum level. Then the signal should remain relatively flat out to a dose of 1×10^{15} ions per cm^2, which means that 10,000 ion beam pulses could be directed at the target after prerastering without significant loss of signal.

We used a robotic printer located at Oak Ridge National Laboratory to deposit Sn-lableled oligos. Figure 7 shows an image of approximately 40-nanoliter spots of ODN-B (respectively 88-μM and 18-μM) deposited by the ORNL robot at 1 mm spacing. These spots and similar scans of Oligos A and C spots show a somewhat bimodal distribution of the robotic deposition which may indicate the nozzle was partly plugged during our deposition and the spots may contain significantly less material than expected.

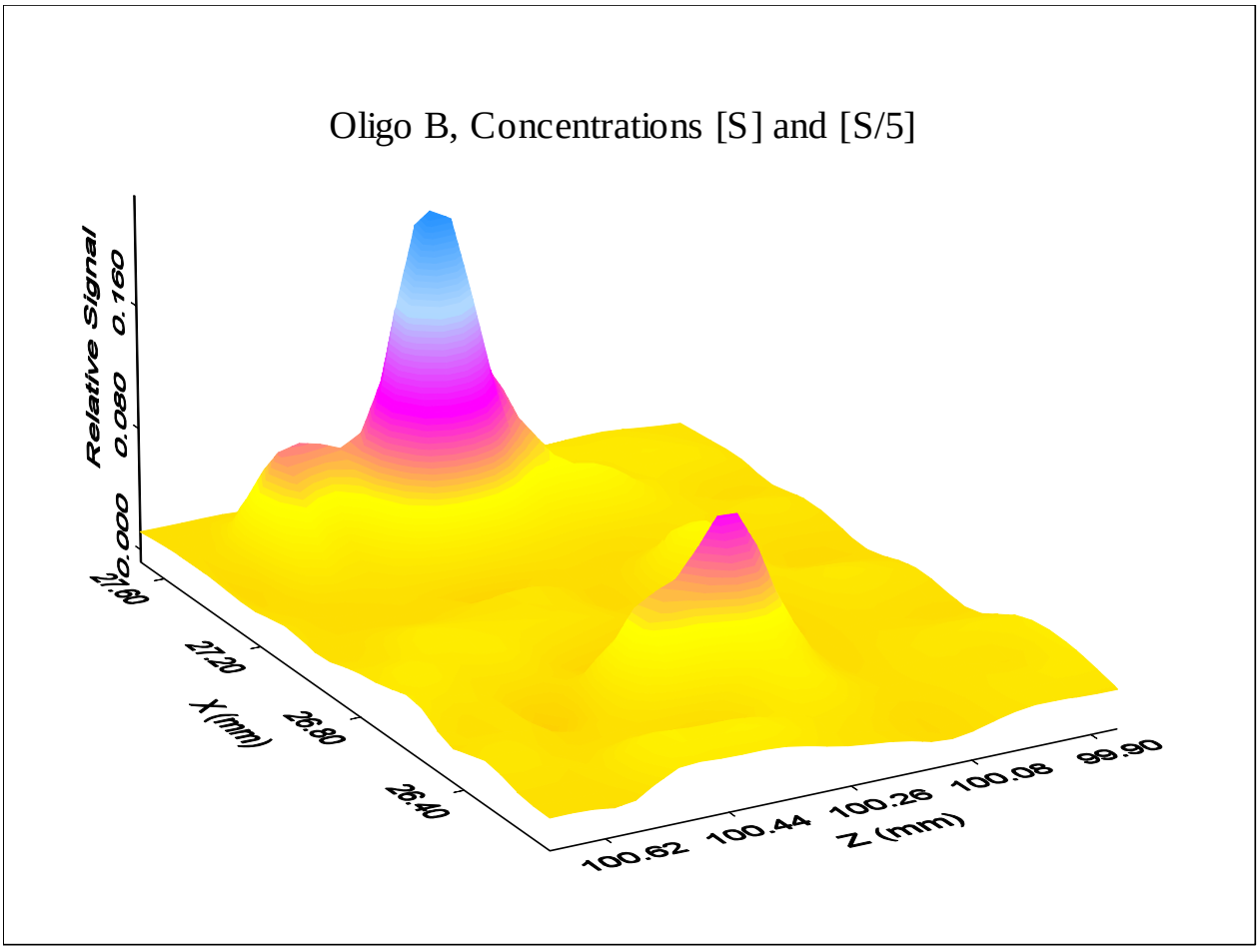

Figure 7. SIRIS image from approximately 40 nanoliter spots, respectively 88 μM and 18 μM, of ODN-B deposited by robotic printer.

We needed a known quantity of material on the surface to calibrate the instrument response for SIRIS analysis of Sn-labeled ODNs so we measured the signal from unwashed Sn-labeled ODN spots deposited by hand pipetting. Even though these were much larger spots than would be used on a microarray (volume = 2 μl), it is one of the few ways to put down a known quantity of material. However, we discovered the signal from the unwashed spots diminished dramatically with time in the vacuum chamber, evidently because the TESPA was volatile. Preparative HPLC had been used to isolate the labeled ODNs from unlabeled ODNs and from unreacted TESPA so we were sure that the deposited material was singly labeled ODNs. We performed similar experiments with washed ODNs. The signal from washed spots also diminished under vacuum but to a lesser degree, leading to the conclusion that not all the labeled ODNs that remained after washing were attached by covalent bonds to the surface. This did not bode well for development of a quantitative analytical method using the Sn-labeled ODNs.

Because of volatility issues, the large background of natural Sn, and the high cost of isotopes of Sn, we were forced to abandon Sn as the label for our oligo measurements. A quick search found several possible alternatives. We discarded the idea of using gold because several components in the SIRIS system are gold plated. Europium and platinum labels were selected for testing.

Europium- and Platinum-Labeled Oligos

50 μg of a Eu-labeled modified oligo was purchased from PerkinElmer Life Sciences;

5'-/5ThioMC$_6$/ACT GCA ACG TCA ACT GCA ACG TCA/Eu – 3'. A 1-μM solution was prepared and a 10-fold dilution series was deposited onto 1-cm x 1-cm silicon wafers coated with 20-40 nm thick gold (coatings produced in-house by a vapor deposition system). A Eu resonance ionization scheme was developed using the energy levels from published tables [29]. The transition from the $^8S^o_{7/2}$ ground state to the $^8P_{9/2}$ at 40,455 cm^{-1} was selected for a single resonance scheme. This was achieved by mixing the output of the Nd:YAG fundamental (1.064 μm) with the frequency doubled output of a dye laser operating at approximately 644 nm. From the upper state, one more photon from the Nd:YAG fundamental will photoionize the Eu atom.

A 10^{-8} molar solution of Eu in EDTA was prepared for use in tuning up the lasers and SIRIS system to the europium signal.

The SIRIS signals for Europium were very small. We are not sure whether this is a result of poor labeling efficiency, poor attachment efficiency to the Si wafers, or incomplete atomization of the Eu from the oligo. At the same time we tested Eu-labeled oligos, we also tested a Pt label, which worked much better and therefore the Eu-labels were abandoned. In order to know how much oligo was deposited on a surface, we developed a dual labeling method that attached ^{33}P and Pt as labels to the same oligo. This technique allowed us to quantitatively determine the amount of oligo on a surface using a BioScan AR-2000 imager (Bioscan, Washington, DC) and then use SIRIS to detect the Pt label.

Dual-labeling Procedure. 2 μg samples of these oligos were labeled with Pt-containing DIG-Chem Link™ (Roche) in 20 μl reactions. The DIG-Chem Link™ (40 $\mu g ml^{-1}$) labeling reactions were incubated at 85°C for 90 min and purified by HPLC. Figure 8 shows a HPLC chromatogram for the Pt-labeled oligo. The conditions for this chromatogram were:

- Column: Waters Xterra RP18; 5 μm 4.6 x 50 mm (Lot# T23081; part # 186000484)
- Solvent A = acetonitrile (ACN)
- Solvent B = 10 % acetonitrile / 90 % 0.1 M TEAA buffer pH 7.0 (v/v)
- Solvent C = 50 % acetonitrile / 50 % 0.1 M TEAA buffer pH 7.0 (v/v)
- Solvent D = water
- Flow Rate: 1 mL/min
- Column Compartment Temperature: 35 oC
- Detection Wavelength: 254 nm and 260 nm
- Injection Volume: 100 μL

Linear Gradient:

Time (min)	%A	%B	%C	%D
0	0	95	5	0
20	0	65	35	0
45	0	65	35	0

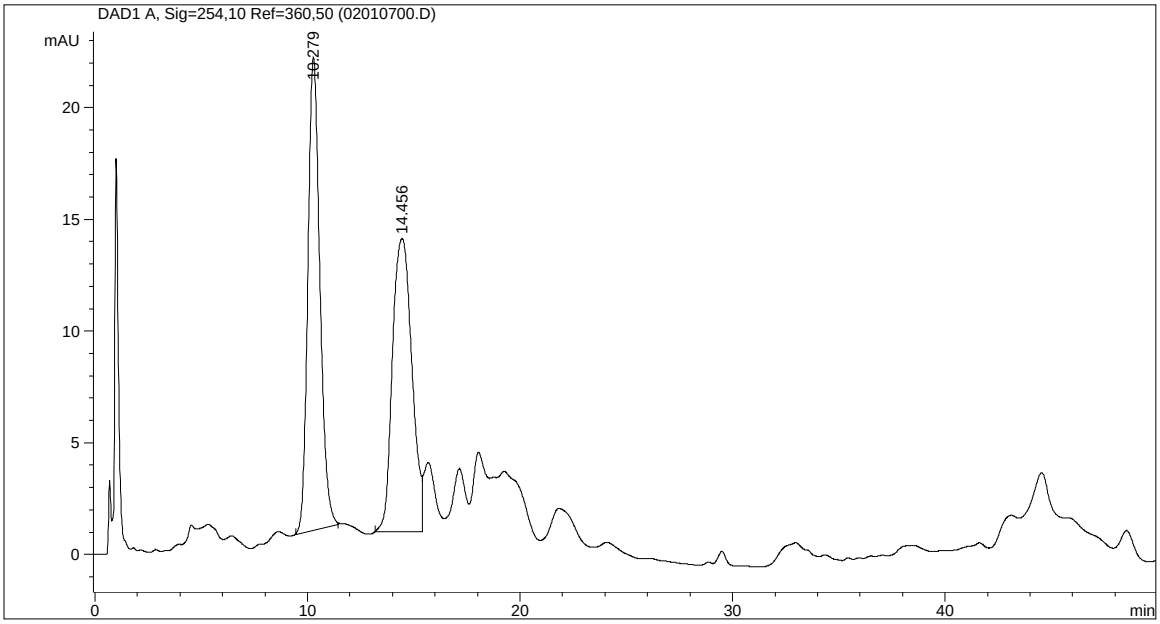

Figure 8. Typical HPLC Chromatogram for platinum-labeled oligos. The first peak, at approximately 10 minutes retention time, is the unlabeled oligo and the second peak, at approximately 14.5 minutes is the singly labeled oligo.

The collected Pt-labeled ODNs were evaporated under vacuum at 43°C overnight, and dissolved in 50 µl ddH_2O. They were then 3'end-labeled with 3 pmol α^{33}P-ddATP (3000 Ci/mmol, ICN) or 3 pmol α^{32}P-ddATP (3000 Ci/mmol), with 100 U terminal transferase (Roche) according to the manufacturer's procedure in 40-µl reaction volumes incubated at 37°C for 3 h. A dideoxy nucleotide was used to insure that a maximum of 1 ^{33}P/ODN would result, thus allowing a direct comparison between SIRIS and the AR-2000 scanner. Alternatively, 3'-thiol modified ODNs were labeled with DIG-Chem Link™ as described above, and 5'-end labeled with ^{33}P using T4 Polynucleotide Kinase (New England BioLabs) and γ^{33}P-ATP (3000 Ci/mmol, ICN). It was determined that ^{33}P was the preferred label because the lower energy beta emission (0.25 MeV for ^{33}P as compared to 1.71 MeV for ^{32}P) and the longer half-life (25.3 days for ^{33}P as compared to 14.3 days for ^{32}P) resulted in less DNA damage.

The labeled ODNs were passed through a 1-cm column of Sephadex G-25 (GE-Healthcare) molecular exclusion resin in a spin filter, adjusted to pH 4.0 with 0.1 volumes of 2 M sodium acetate, and cleared of protein by extraction with phenol chloroform isoamyl alcohol (25:24:1) and centrifugation at 6000 × g for 10 min. The organic phase was re-extracted by additions of 50 µl 200 mM sodium acetate pH 4.0, vortexing the mixture and centrifuging as

described above. Following the second centrifugation, 50 µl of the organic phase was deposited in a Petri dish and determined not to contain disintegrations above background using a hand held rate meter. The purified ODNs were precipitated overnight with 3 volumes ethanol and centrifuged at 16,000 × g for 20 min, and dissolved in 20 µl ddH_2O. The ethanol solution from ODN precipitation was checked for radioactivity and found to not contain counts above background indicating that unincorporated label was efficiently removed by the molecular-exclusion resin. The amount of dual-labeled ODN required to gain reproducible counts at least 3-fold above background was determined using 1-µl aliquots from a 2-fold dilution series deposited into 2 mm wells of a Teflon® Printed Slide (Erie Scientific) and measured with the AR-2000 using a 5 min count. Figure 9 below shows an AR-2000 scan over a dilution series for an 18-mer.

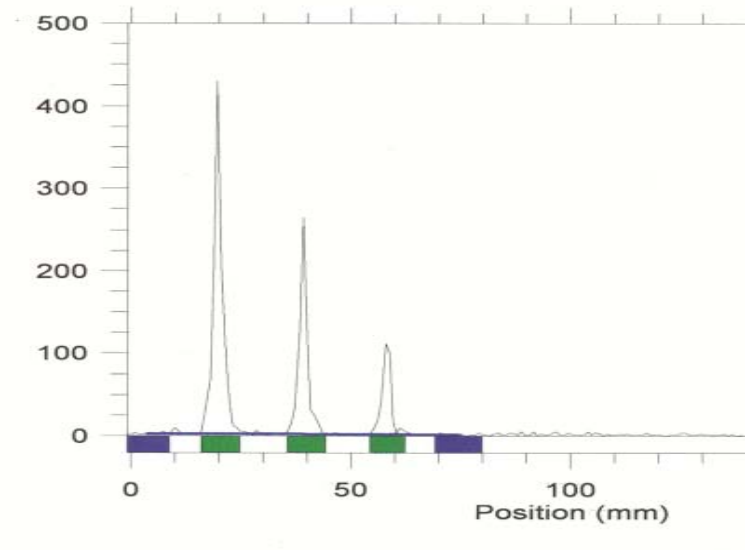

Immobilization of dual-labeled ODNs onto MPTS treated silicon. 1 cm square silicon wafers (Silicon Inc., Boise Idaho) were treated at 80°C for 1 h in a solution of 5% H_2O_2 and 30% ammonium hydroxide and rinsed under a constant stream of ddH_2O. The wafers were transferred to a borosilicate glass bottle containing 1% 3-mercaptopropyl-trimethoxy silane (MPTS) in absolute ethanol. The silicon wafers were removed from the silanization solution, rinsed with absolute ethanol, baked at 108°C for 1 h, and stored under vacuum until used.

To determine immobilization efficiency and establish immobilization density, 100 nl aliquots of the labeled probes were deposited using a Hamilton 7000 Series Modified

Microliter™ syringe and allowed to immobilize until the deposited volume had dried. The chips were then counted prior to washing. The chips were washed by floating the silicon wafers (printed side down) on 3 successive 20 ml volumes of 18 MΩ ddH_2O on petri dishes and counted again to determine immobilization density of the Pt labeled probes.

We then ran a series of SIRIS images of the same spots, monitoring the Pt label. The figures below show three images of a spotted 40-mer taken with 25 frames of ion-beam rastering between each image.

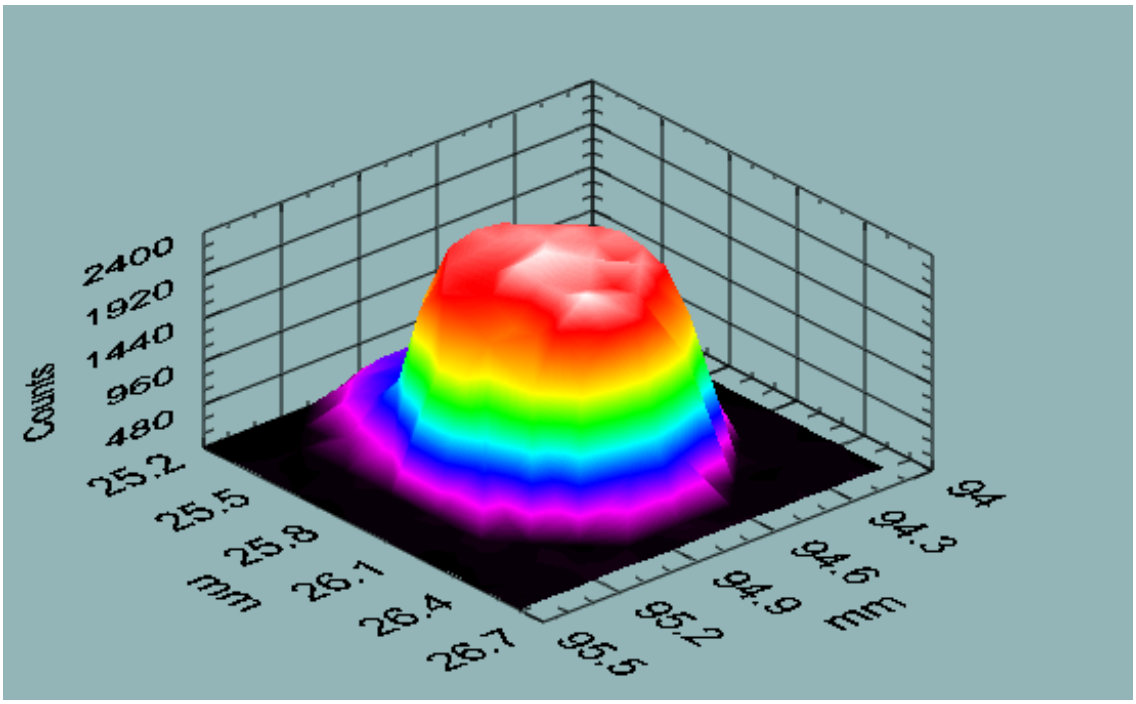

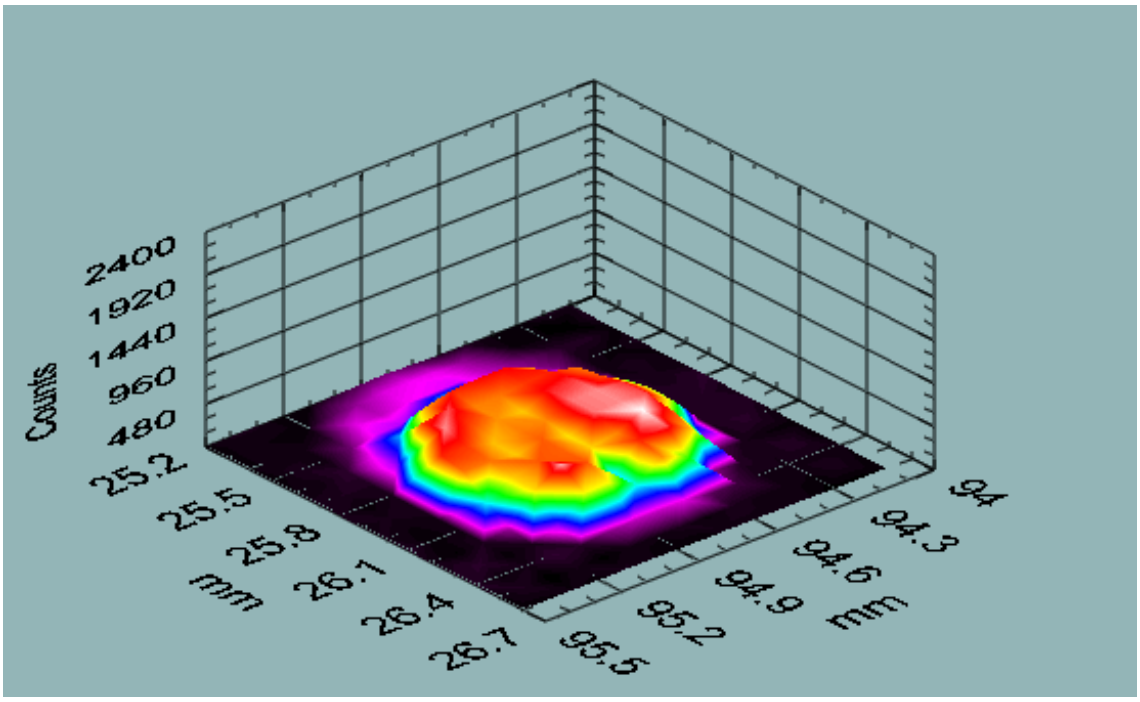

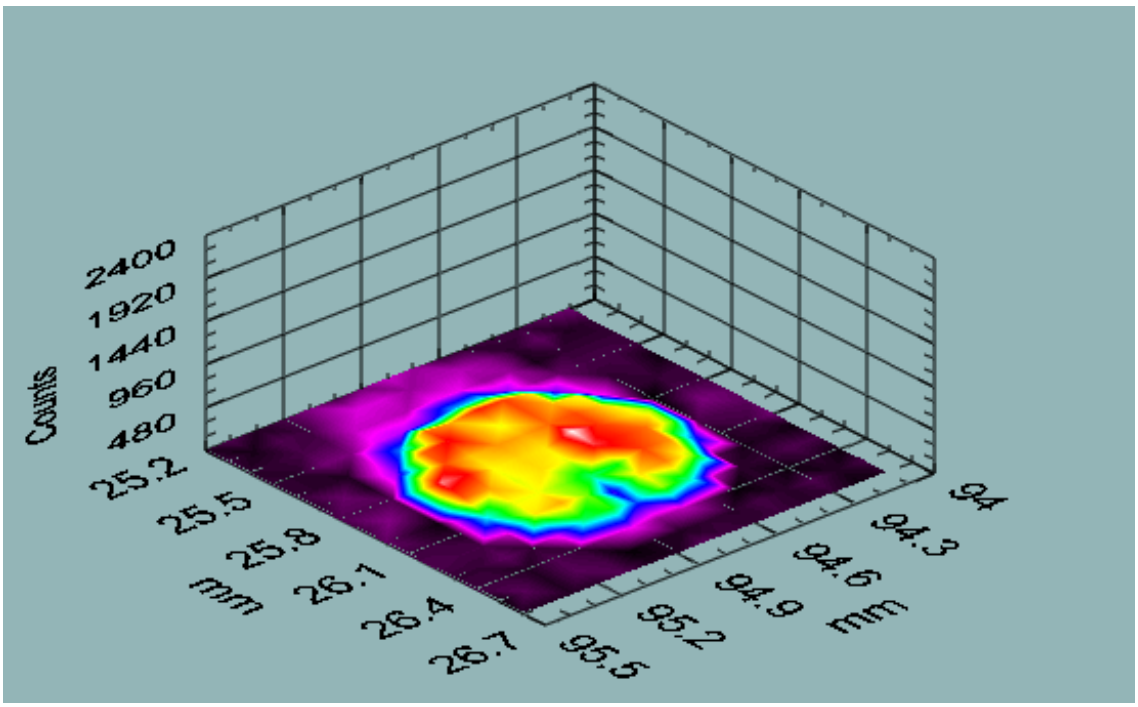

The ion beam dose that provided these images is known as is the dose of each raster frame. Therefore, we can calculate the equivalent signal for the Pt label over the entire three-dimensional spot. This data pointed out that we should take smaller steps than 25 raster frames between images so we will

have better "depth" resolution and a more accurate integration of the amount of platinum in the spot. We were in the process of doing this for an 18-mer and a 40-mer dilution series when the SIRIS instrument failed. It took several weeks to repair the SIRIS instrument.

When the SIRIS instrument was repaired, we returned to experiments to compare the SIRIS signal to the AR-2000 signal for double-labeled oligos. We had observed some indication that the position of the label might influence the SIRIS signal so we had oligos synthesized with a single guanidylate positioned proximal, medial, and distal to a 5' thiol-C_6 linker. Discussions with Roche Applied Science indicated that the DIG-Chem Link™ reagent results in attaching a single complexed Pt at each G residue.

In Figure 10, four oligos were immobilized on Si wafers as described above.

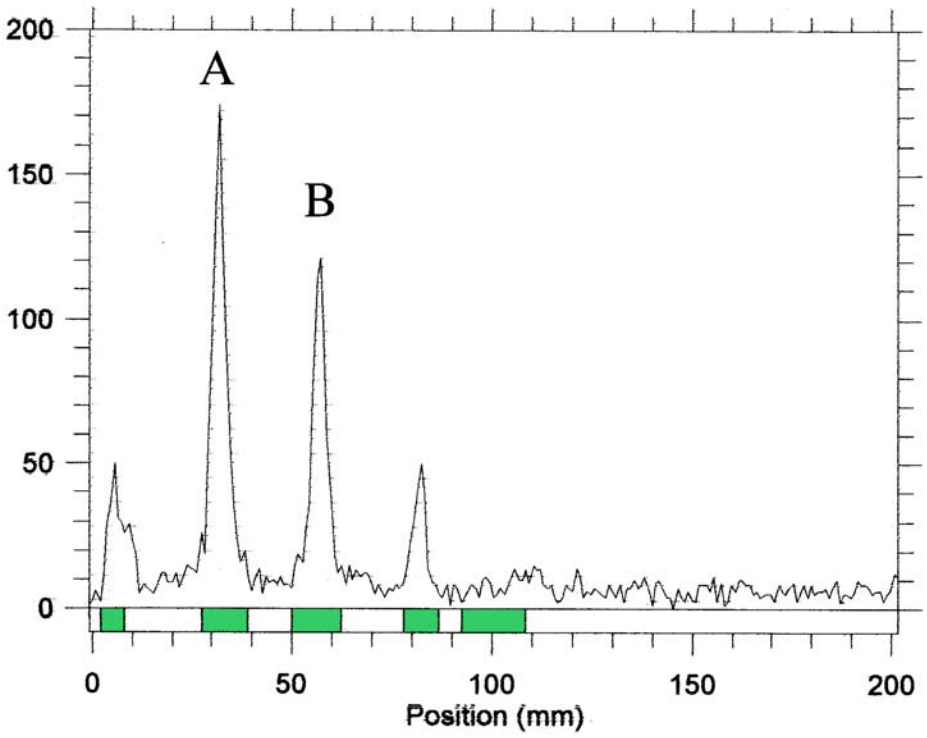

Figure 10. AR-2000 scan of 18-mer oligos labeled with both Pt and ^{33}P. Peak A had the Pt label attached in the central portion of the oligo and Peak B had Pt attached away from the 5' linker.

Peak A is an 18mer with medial G. Peak B is an 18mer with distal G. The peak to the left of Peak A is an 18mer with proximal G. An examination of the the proximal G Peak (to the left of

A) shows that is not used in subsequent calculations because of the small number of counts and the strange peak shape. The peak to the right of Peak B is a 32mer used for length comparisons.

	Proximal	Medial (Peak A)	Distal (Peak B)
Integrated # Counts (AR-2000)	188*	875	646
Integrated SIRIS Signal		46089	51101
Ratio SIRIS/AR-2000		52.7	79.1

SIRIS data was integrated over all isotopes of Pt and over a 1 mm x 1 mm area rastered in 0.1 mm steps.

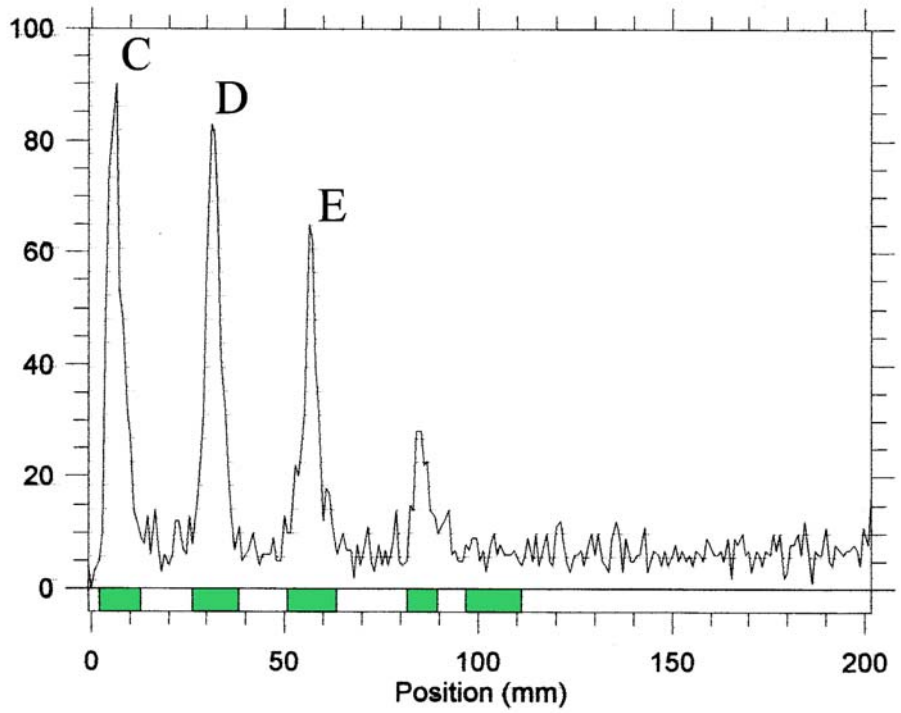

Figure 11. Similar to Figure 10. AR-2000 scan of 18-mer oligos labeled with both Pt and ^{33}P. Peak C had the Pt label attached near the 5' linker. Peak D had Pt attached at the middle portion of the oligo. Peak E had Pt attached away from the 5' linker.

	Proximal	Medial (Peak A)	Distal (Peak B)
Integrated # Counts (AR-2000)	498	482	376
Integrated SIRIS Signal	51,414	102,819	64,995
Ratio SIRIS/AR-2000	103.2	213.3	172.8

Conclusions – Clearly the SIRIS signal does not give a signal proportional to the amount of oligo attached to the surface as determined by the decay of the ^{33}P label. SIRIS has been shown to be an excellent technique for quantitative measurements of several types of samples so the question arises as to what is different here. We intentionally tested conditions under which one might expect the atomization efficiency to change and we believe this is the problem. Different lengths of oligos, and different placement of the label in the oligo affected the final signal. This obviously makes use of SIRIS as a quantitative tool for oligonucleotides problematic except under highly controlled situations.

1. D.F. Easton, D.T. Bishop, D. Ford, G.P. Crockford, and the Breast Cancer Linkage Consortium, American Journal of Human Genetics **52**, 678 (1993).
2. W. Bains, GATA **11**, 49 (1994).
3. K.L. Beattie, W.G. Beattie, L. Meng, S.L. Turner, R. Coral-Vazquez, D.D. Smith, P.M. McIntyre and D.D. Dao, clinical Chemistry **41**, 700 (1995).
4. C.D. Bain, E.B. Troughton, T. Tao, J. Evall, G.M. Whitesides, and R.G. Nuzzo, The Journal of the American Chemical Society **111,** 321 (1989).
5. W. Feldman and P. Pevzner, Genomics **23**, 233 (1994).
6. Z. Guo, R.A. Guilfoyle, A.J. Thiel, R. Wang and L.M. Smith, Nucleic Acids Research **22**, 5456 (1994).
7. S.P.A. Fodor, J.L. Read, M.C. Pirrung, L. Stryer, A.T. Lu, and D. Solas, Science **251**, 767-773 (1991).
8. J.G. Hacia, L.C. Brody, M.S. Chee, S.P.A. Fodor and F.S. Collins, Nature Genetics **14**, 441-447 (1996).
9. A.P. Shuber, J. Skoletsky, R. Stern, and B.L. Handelin, Human Molecular Genetics **2**, 153 (1993).
10. J.M. DeMarchi, C.S. Richards, R.G. Fenwick, R. Pace and A.L. Beaudet, Human Mutation **4**, 282 (1994).
11. D.I. Lewin, The Journal of NIH Research **7**, 38 (1995).
12. P. Aldous, New Scientist **144**, 8 (1994).
13. M. Sjöroos, A. Iitiä, J. Ilonen, H. Reijonen and T. Lövgren, BioTechniques **18**, 870 (1995).
14. K.L. Beattie, W.G. Beattie, L. Meng, S.L. Turner, R. Coral-Vazquez, D.D. Smith, P.M. McIntyre and D.D. Dao, clinical Chemistry **41**, 700 (1995).

15. C.D. Bain, E.B. Troughton, T. Tao, J. Evall, G.M. Whitesides, and R.G. Nuzzo, The Journal of the American Chemical Society **111,** 321 (1989).
16. W. Feldman and P. Pevzner, Genomics **23**, 233 (1994).
17. Z. Guo, R.A. Guilfoyle, A.J. Thiel, R. Wang and L.M. Smith, Nucleic Acids Research **22**, 5456 (1994).
18. S.P.A. Fodor, J.L. Read, M.C. Pirrung, L. Stryer, A.T. Lu, and D. Solas, Science **251**, 767-773 (1991).
19. A. Marshall and J. Hodgson, Nature Biotechnology **16**, 27 (1998).
20. H.F. Arlinghaus, M.N. Kwoka, X.-Q. Guo and K.B. Jacobson, Analytical Chemistry **69**, 1510 (1997).
21. H.F. Arlinghaus, M.N. Kwoka and K.B. Jacobson, Analytical Chemistry **69**, 3747 (1997).
22. K.B. Jacobson and H.F. Arlinghaus, Anal. Chem. **64**, 315A (1992).
23. H.F. Arlinghaus and C.F. Joyner, J. Vac. Sci. Technol. **B14 (1),** 294 (1996).
24. H.F. Arlinghaus, T.J. Whitaker, C.F. Joyner, M. Kwoka, K.B. Jacobson, and J. Tower, in Proceedings SIMS X, A. Benninghoven, B. Hagenfhoff, H.W. Werner, Eds.; John Wiley and Sons: New York, 123-130 (1997).
25. N. Thonnard, J.E. Parks, R.D. Willis, L.J. Moore, and H.F. Arlinghaus, Surf. Interface Anal. **14**, 751 (1989).
26. F.V. Sloop, G.M. Brown, R.S. Foote, K.B. Jacobson and R.A. Sachleben, Bioconjugate Chemistry **4**, 106 (1993).
27. S. Agrawal, C. Christodoulou and M.J. Gait, Nucleic Acids Research **14**, 6227 (1986).
28. R.J. Kaiser, S.L. MacKellar, R.S. Vinayak, J.Z. Sanders, R.A. Saavedra and L.E. Hood, Nucleic Acids Research **17**, 6087 (1989).
29. Atomic Energy Levels – The Rare-Earth Elements, edited by W.C. Marin, Romuald Zalubas, and Lucy Hagan, National Bureau of Standards (NSRDS-NBS 60), 1978.